Ramos *et al. Geosci. Lett. (2017) 4:12*
DOI 10.1186/s40562-017-0078-3

Geoscience Letters

RESEARCH LETTER



# Occurrence of 1 ka-old corals on an uplifted reef terrace in west Luzon, Philippines: Implications for a prehistoric extreme wave event in the South China Sea region

Noelynna T. Ramos[1*], Kathrine V. Maxwell[1], Hiroyuki Tsutsumi[2], Yu-Chen Chou[3], Fucai Duan[3], Chuan-Chou Shen[3] and Kenji Satake[4]

**Abstract**

Recent $^{230}$Th dating of fossil corals in west Luzon has provided new insights on the emergence of late Quaternary marine terraces that fringe west Luzon Island facing the Manila Trench. Apart from regional sea level changes, accumulated uplift from aseismic and seismic processes may have influenced the emergence of sea level indicators such as coral terraces and notches. Varied elevations of middle-to-late Holocene coral terraces along the west Luzon coasts reveal the differential uplift that is probably associated with the movement of local onland faults or upper-plate structures across the Manila Trench forearc basin. In Badoc Island, offshore west of Luzon mainland, we found notably young fossil corals, dated at 945.1 ± 4.6 years BP and 903.1 ± 3.9 years BP, on top of a ~5-m-high reef platform. To constrain the mechanism of emergence or emplacement of these fossil corals, we use field geomorphic data and wave inundation models to constrain an extreme wave event that affected west Luzon about 1000 years ago. Our preliminary tectonic and tsunami models show that a megathrust rupture will likely lead to subsidence of a large part of the west Luzon coast, while permanent coastal uplift is attributed to an offshore upper-plate rupture in the northern Manila Trench forearc region. The modeled source fault ruptures and tsunami lead to a maximum wave height of more than 3 m and inundation distance as far as 2 km along the coasts of western and northern Luzon. While emplacement of coral boulders by an unusually strong typhoon is also likely, modeled storm surge heights along west Luzon do not exceed 2 m even with Typhoon Haiyan characteristics. Whether tsunami or unusually strong typhoon, the occurrence of a prehistoric extreme wave event in west Luzon remains an important issue in future studies of coastal hazards in the South China Sea region.

**Keywords:** Coral terraces and boulders, $^{230}$Th dating, Prehistoric extreme wave event, Coastal hazards, South China Sea region, Philippines

## Background

Coastal zones are among the most vulnerable in the world because of their exposure to sea level fluctuations brought about by climate conditions, tropical cyclones, and tectonic processes. The Asia-Pacific region, in particular, is constantly affected by extremely strong waves brought about by tsunamis (e.g., 2011 Tohoku-oki earthquake in Japan) and super typhoons (e.g., 2013 Typhoon Haiyan in the Philippines) [e.g., (Terry and Goff 2012)]. Of particular interest in the Southeast Asian region is the tsunami-generation potential of the Manila Trench which poses risks to coastal zones across the South China Sea (SCS). Over the years, the tsunami-generation potential of the Manila Trench has been highlighted in the tsunami hazard assessments of Taiwan, Thailand, China, Vietnam, Malaysia, Singapore, and Philippines [e.g., (Dao

*Correspondence: noelynna.ramos@up.edu.ph
[1] National Institute of Geological Sciences, College of Science, University of the Philippines, Diliman, 1101 Quezon City, Philippines
Full list of author information is available at the end of the article

et al. 2009; Huang et al. 2009; Liu et al. 2009; Megawati et al. 2009; Ruangrassamee and Saelem 2009; Wu and Huang 2009; Nguyen et al. 2014; Li et al. 2016)]. In the Philippines, recent efforts in tsunami studies involve characterization of source faults through validation of historical and modern tsunami observations [e.g., (Bautista et al. 2012; Salcedo 2014)]. Mapping and radiometric dating of emergent coral terraces and coral microatolls are also being done to understand the active tectonics of the Manila Trench and its associated upper-plate tectonic structures [e.g., (Ramos and Tsutsumi 2010; Abigania 2011)]. We found ~1000-year-old coral debris on an island, approximately 120 km offshore west Luzon mainland, to be particularly interesting because of their implications for regional coastal hazards at the millennial scale. In the west Pacific, transported reef-platform coral boulders offer important insights into the occurrence of extreme wave events such as tsunamis or strong typhoons [e.g., (Yu et al. 2004; Goto et al. 2010; Terry and Etienne 2014; May et al. 2015)]. In this study, we use emergent coral terraces, fossil coral data (e.g., elevation, $^{230}$Th age), and numerical modeling to constrain a prehistoric extreme wave event along the northern Manila Trench forearc region about 1000 years ago that could potentially be larger than those recorded in the almost 400-year-long written history of the Philippines.

## Seismotectonic setting and geomorphologic background

The oppositely dipping subduction zones in the Philippines are among the least-studied and least-constrained active megathrust zones in Southeast Asia. The east-dipping discontinuous Manila–Negros–Sulu–Cotabato Trench system and the west-dipping Philippine Trench system are potential sources of large magnitude offshore earthquakes which pose imminent threats to lives and properties along coastal communities (Li et al. 2016; Ramos and Tsutsumi 2010; Besana et al. 2004; Fig. 1). Of the trench systems in the archipelago, the Manila Trench has received much attention due to its seismic potential and the tsunami hazard it poses to coastal megacities surrounding the South China Sea. In the last 400 years of historical records and instrumental seismicity in the Philippines, the largest earthquakes that are possibly associated with the Manila Trench occurred in 1852 (Ms7.6) and 1934 (Ms7.6) (Bautista et al. 2012) (Fig. 1c).

As the archipelago is lined with thousands of kilometers of coastline, the impacts of coastal flooding brought about by extreme wave events remain one of the biggest concerns during this time of increasing surface temperatures and sea level [e.g., (Intergovernmental Panel on Climate Change (IPCC) 2013; Villarin et al. 2016)]. Aside from the threat of tsunamis, coastal communities around the SCS region are also at risk from the impacts of extreme weather events such as storm surges. Coastal geomorphic features such as coral-reef platforms and solution notches provide us opportunities not only to better understand the mechanisms and processes of coastal hazards but also to prepare for their impacts.

## Methods

### Field surveys and interpretation of remote sensing data

Prior to surveys, aerial photographs and satellite images were studied to identify coasts with well-preserved geomorphic features. Aerial photographs of 1:16,000-scale and 5-m Interferometric Synthetic Aperture Radar (IFSAR)-derived topographic data were sourced from the National Mapping and Resource Information Authority (NAMRIA) in the Philippines. We also used Google Earth images to delineate the boundaries of local geomorphic units. Fossil corals, presumably fresh and pristine, were then collected from emergent platforms whenever available. Topographic profiles of emerged coastal features were generated using a TruPulse 360 R rangefinder and a tripod. We measured the elevation of the paleoshoreline angle and/or inner edge of coral platforms from the tide level at the time of survey, then corrected for mean sea level at the nearest tide gauge station (i.e., Currimao). We use 'inner edge' when the shoreline angle (i.e., junction between the cliff and abrasion platform) is obscured by overlying colluvium or beach deposits [e.g., (Jara-Muñoz et al. 2015)]. The elevations of terrace surfaces and their associated inner edge, or shoreline angle when observed, are reported in meters above mean sea level (m amsl). Mean sea level along the northwestern coasts of Luzon Island ranges from 0.24 to 0.33 m as recorded in two tide gauge stations (Currimao and San Fernando), while tidal range is 0.54 to 0.68 m (National Mapping and Resource Information Authority (NAMRIA) 2016).

### $^{230}$Th dating

Five fossil coral samples from one survey site in northern Badoc Island were analyzed for $^{230}$Th dating (Shen et al. 2012). U-Th isotopic compositions of the selected chipped subsamples, which were gently crushed and physically cleaned with ultrasonic methods (Shen et al. 2008), were determined on a multicollector inductively coupled plasma mass spectrometer (MC-ICP-MS), Thermo Fisher Neptune (Shen et al. 2012). Recent data on half-lives of U-Th nuclides were used to calculate the $^{230}$Th ages of the samples (Shen et al. 2012). Uncertainties in the U-Th isotopic data and $^{230}$Th dates relative to 1950 AD (years BP) are given at the two-sigma (2σ) level or two standard deviations of the mean ($2\sigma_m$) unless otherwise noted. U-Th chemistry (Shen et al. 2003) and

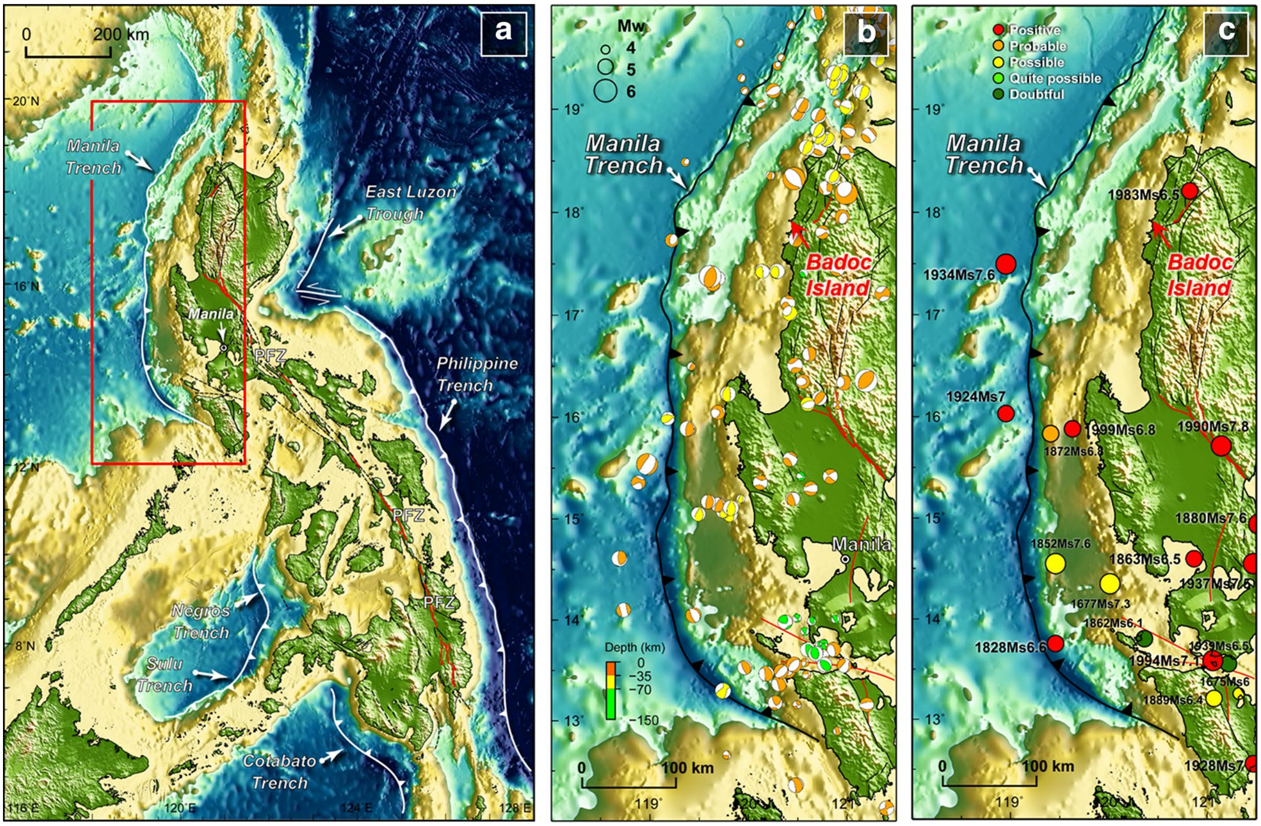


**Fig. 1** **a** Tectonic setting of the Philippine archipelago showing surrounding subduction zones. **b** Focal mechanism solutions (FMS) (1976–2017) show generally shallow fault activities related to structures along the Manila Trench and onland segments of the Philippine Fault (Tsutsumi and Perez 2013; Philippine Institute of Volcanology and Seismology (PHIVOLCS) 2015). Reported active faults are shown in red. FMS data are from the Global Centroid Moment Tensor (GCMT) catalog. **c** Tsunami events in west Luzon Island have often been associated with Ms6 to Ms7 earthquakes along the Manila Trench. Tsunamigenic earthquakes that affected west Luzon are shown in Table 4 with their probability ranking and maximum wave height (Bautista et al. 2012)

instrumental analysis (Shen et al. 2012) were conducted at the High-Precision Mass Spectrometry and Environment Change Laboratory (HISPEC), National Taiwan University.

The analyzed U-Th isotopic compositions and contents of the samples presented here are given in Table 1. The absence of secondary carbonates in the intraskeletal structure, the $^{238}$U levels of 2.3–3.4 ppm, and the initial $\delta^{234}$U values of 143.8-148.1‰ as in modern corals and seawater (Shen et al. 2008) suggest that the selected coral samples are well preserved. $^{230}$Th ages of fossil corals range from 6871.7 ± 22 years BP to 903.2 ± 3.9 years BP and possibly represent the timing of emergence of reef platforms brought about by global mean sea level changes and tectonic processes from middle to late Holocene.

## Numerical modeling

The geometric characteristics of modeled fault ruptures along the northern Manila Trench forearc region were assumed from seismicity patterns, earthquake focal mechanisms, geophysical data, and coseismic deformation inferred from uplifted coral terraces [e.g., (Ramos and Tsutsumi 2010; Hayes and Lewis 1984)]. Source fault parameters and resulting surface deformation were then established using scaling relations for subduction zone earthquakes, upper-plate faults, and elastic dislocation models (Okada 1985; Murotani et al. 2013; Wells and Coppersmith 1994) (Table 2), while also considering the effect of bathymetry and horizontal displacement (Tanioka 1996).

Tsunami modeling was performed using JAGURS, a numerical code that computes tsunami propagation and inundation on the basis of the long waves or the dispersive waves (Boussinesq-type) [e.g., (Satake 2002; Saito et al. 2010; Baba et al. 2015)]. For near-field tsunamis, the code takes into account the effects of horizontal displacement and seafloor slope [e.g., (Tanioka 1996)]. These are solved on a finite difference scheme using a staggered

**Table 1 U-Th isotopic compositions and $^{230}Th$ ages for corals of Badoc Island by MC-ICPMS, Thermo Electron Neptune, at HISPEC, NTU**

| Sample ID | Weight g | $^{238}U$ ppb[a] | $^{232}Th$ ppt | $d^{234}U$ measured[a] | $[^{230}Th/^{238}U]$ activity[c] | $^{230}Th/^{232}Th$ atomic ($\times 10^{-6}$) | Age (year ago) uncorrected | Age (year ago) corrected[c,d] | Age (year BP) relative to 1950 AD | $\delta^{234}U_{initial}$ corrected[b] |
|---|---|---|---|---|---|---|---|---|---|---|
| BAD-071914-2.1 | 0.26321 | 2324.0 ± 3.6 | 30.3 ± 1.8 | 145.2 ± 2.2 | 0.07067 ± 0.00017 | 89,269 ± 5199 | 6937 ± 22 | 6936 ± 22 | 6871.7 ± 22 | 148.1 ± 2.2 |
| BAD-071914-2.2 | 0.20931 | 3151.7 ± 4.7 | 595.6 ± 2.6 | 147.2 ± 2.1 | 0.010623 ± 0.000038 | 926.8 ± 5.0 | 1014.3 ± 4.1 | 1009.9 ± 4.6 | 945.1 ± 4.6 | 147.6 ± 2.1 |
| BAD-071914-2.3 | 0.21320 | 3130.4 ± 5.1 | 161.0 ± 2.2 | 143.4 ± 2.3 | 0.010119 ± 0.000035 | 3245 ± 46 | 969.2 ± 3.9 | 968.0 ± 3.9 | 903.1 ± 3.9 | 143.8 ± 2.3 |
| BAD-022215-09 | 0.10863 | 2564.8 ± 2.4 | 27.5 ± 4.3 | 144.8 ± 1.4 | 0.0145 ± 0.0001 | 22293 ± 3471 | 1387 ± 5 | 1386.6 ± 5.4 | 1320 ± 5 | 145.4 ± 1.4 |
| BAD-111815-01 | 0.14431 | 3374.9 ± 2.9 | 69.6 ± 3.2 | 145.4 ± 1.3 | 0.02898 ± 0.00013 | 23170 ± 1079 | 2793 ± 13 | 2793 ± 13 | 2727 ± 13 | 146.6 ± 1.4 |

Decay constants are $9.1705 \times 10^{-6}$ $year^{-1}$ for $^{230}Th$, $2.8221 \times 10^{-6}$ $year^{-1}$ for $^{234}U$ (Cheng et al. 2013), and $1.55125 \times 10^{-10}$ $year^{-1}$ for $^{238}U$ (Jaffey et al. 1971)

[a] $[^{238}U] = [^{235}U] \times 137.77$ (±0.11‰) (Hiess et al. 2012); $\delta^{234}U = ([^{234}U/^{238}U]_{activity} - 1) \times 1000$

[b] $\delta^{234}U_{initial}$ corrected was calculated based on $^{230}Th$ age ($T$), i.e., $\delta^{234}U_{initial} = \delta^{234}U_{measured}\, X\, e^{\lambda 234*T}$, and $T$ is corrected age

[c] $[^{230}Th/^{238}U]_{activity} = 1 - e^{-\lambda 230T} + (\delta^{234}U_{measured}/1000)[\lambda_{230}/(\lambda_{230} - \lambda_{234})](1 - e^{-(\lambda 230 - \lambda 234)\,T})$, where $T$ is the age

[d] Age corrections, relative to chemistry date, were calculated using an estimated atomic $^{230}Th/^{232}Th$ ratio of 4 (±2) $\times 10^{-6}$ (Shen et al. 2008)

**Table 2 Fault parameters used in the rupture and tsunami models**

| Model[a] | Long (°E) | Lat (°N) | Length (km) | Width (km) | Depth (km) | Strike (°) | Dip (°) | Rake (°) | Slip (m) | $M_w$ |
|---|---|---|---|---|---|---|---|---|---|---|
| 1 | 119.3 | 14 | 440 | 120 | 2 | 0 | 15 | 90 | 3.5 | 8.5 |
| 2 | 119.65 | 16 | 400 | 80 | 2 | 18 | 20 | 90 | 5 | 8.4 |

[a] 1-megathrust fault; 2-upper-plate fault

grid and the leapfrog method [e.g., (Jakeman et al. 2010; Baba et al. 2014; Baba et al. 2015)]. We then assume tectonic deformation and tsunami inundation based on geomorphic data available. The tsunami simulation in west Luzon utilized the global 1 arc-min bathymetric grid of Sandwell and Smith (1997) and 1 arc-second topographic grid derived from the Shuttle Radar Topography Mission (SRTM).

## Geomorphology and coastal tectonics of Badoc Island

### Late Quaternary marine terraces

Badoc Island is a small coral island located approximately 1 km off the coasts of west Luzon and approximately 130 km east of the Manila Trench. The coral island is characterized by emergent reef platforms and surrounded by modern fringing reefs. Coral boulders and pedestals resting on the emergent and modern reefs are also dominant along the west coast of the island (Fig. 2). The topmost, cliff-forming reefs that are soil-mantled with elevations ranging from 20 to 28 m are inferred to be of Late Pleistocene age based on the broad, flat morphology resembling an extensive carbonate platform. The Late Pleistocene terrace (LPT) surface is characterized by a thick soil cover with evident landslide scarps, dense grass vegetation, and sporadic occurrence of highly weathered coral heads (Fig. 2a). At the western side of the island facing the South China Sea, the LPT cliff rises up to 28 m amsl, while at the eastern coast, the LPT margin exhibits a broad gently sloping surface that rises from 7 to 20 m amsl.

The Holocene terraces are marked by low-lying (i.e., 2–7 m amsl) sequences of coral reef terraces that are variably preserved and exposed around Badoc Island. We observed up to possibly four Holocene terrace steps with the highest terrace rising up to about 7 m amsl. Along the west coast, coral terraces generally expose rocky and abrasional platforms, while terraces along the northeast and east coasts are often covered with sand and coral debris (e.g., shingle, boulders, broken fragments). The number of terraces as well as the terrace elevations varies around the island. Along the east coast, two to four Holocene terrace steps are observed with Terrace 1 (T1) being the lowest terrace at 1.9–3.7 m amsl, Terrace 2 (T2) at 3–3.8 m amsl, Terrace 3 (T3) at 5.3 m amsl, and Terrace 4 (T4) as the highest terrace rising up to ~7 m amsl. Along the western coast, one to three Holocene terrace steps are observed with T1 measured to be at 2.3–3.4 m amsl, T2 at 3.1–3.8 m amsl, and T3 at 4.6 m amsl; a wave-cut notch was also observed at 5.4 m amsl. New $^{230}$Th ages of fossil corals sampled on top of the terrace surfaces reveal episodes of emergence or relative sea level (RSL) fall during middle to late Holocene. Holocene coral platforms on the northern coasts are generally well preserved with intact fossil corals but their paleoshoreline angle is often obscured by erosion, collapse, or sand deposits. Based on the varied heights of Holocene terraces around the island, tilting to the southeast is suggested (Fig. 2a). Limestone beds and coral debris that comprise the LPT were also noted to be southeast dipping.

Unusual terrace chronology was revealed from fossil coral ages at one survey site in northern Badoc Island, where possibly three terrace steps were recognized: T1 at 2.7 m amsl, T2 at 3.7 m amsl, and T3 at 4.9 m amsl (Fig. 2). The lowest terrace (T1) surface is an abrasional platform exposing massive and eroded corals, and cemented coral rubble. We interpret T1 to be an erosional surface of the mid-Holocene sea level highstand based on the age (6872 ± 22 years BP) of the coral sampled. Meanwhile, a younger (2727 ± 13 years BP) fossil coral was sampled from the terrace riser slope above T2. Unlike T1 which exposes the rocky carbonate platform, the T2 surface is buried by coral boulders and sand. Terrace 3 (T3) is characterized by an almost 60-m-wide subhorizontal surface that is buried by sand, shells and shell fragments, and coral boulders (Fig. 3). Coral boulders are generally distributed just above T2 and the sloping riser separating T2 and T3; individual corals are mostly cm-sized, while a few isolated large blocks are almost a meter wide. The largest coral boulders are often cemented fragments of branching corals (possibly *Acropora*) that similarly comprise the lowest erosional terrace, hence they are assumed as transported blocks from the reef crest. T3 is particularly interesting because notably young (945.1 ± 4.6 years BP and 903.1 ± 3.9 years BP) fossil corals lie within the coral boulder field (Fig. 3; Table 3). The young fossil corals, which appear to be encrusting forms, are approximately 20–30 cm in diameter and 2–5 cm-thick. Although preserved in their upright position, the occurrence of encrusting corals with variably sized

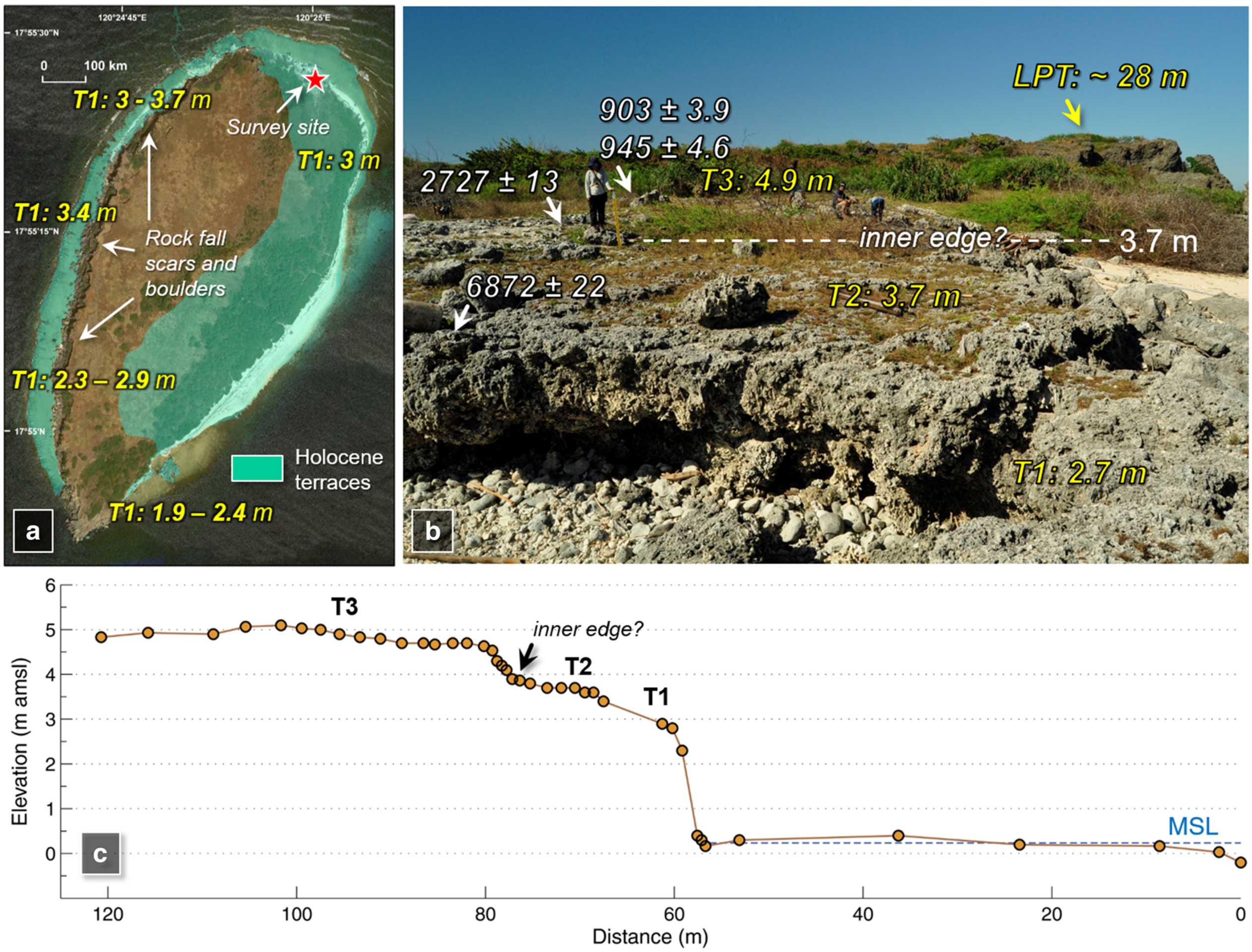


**Fig. 2** Geomorphic features in Badoc Island. **a** Emergent Holocene terraces and fringing reefs surround the island. *Numbers* indicate varied elevations of the lowest terrace, in which higher T1 surfaces are observed to the northwest. The island is inferred to be slightly tilted to the southeast based on variable T1 elevations. **b** At one site to the north, possibly three Holocene terrace surfaces were recognized and these rise up to about 5 m amsl. Elevations (meters above mean sea level, m amsl) and $^{230}$Th ages (relative to 1950 AD, years BP) of fossil corals collected are shown in *white* and *yellow*, respectively. Highest reef platforms at about 20-28 (possibly rising up to ~35) m amsl are inferred to represent the Late Pleistocene terraces (LPT). **c** Topographic profile at the survey site showing the measured elevations of the terraces and *inner edge*, when observed. Mean sea level (MSL) (*blue dashed line*) is 0.24 m and is derived from actual tide data of NAMRIA

overturned boulders of massive corals and cemented coral rubble imply that they are probably allochthonous. The foraminifera-rich coarse sand cover that occurs with the coral debris and buries the upper terraces also implies high-energy deposition [e.g., (Switzer et al. 2010)]. Typically, the age of corals attached on terrace surfaces will have a 'younging' trend as terraces become closer to the present sea level, indicating the most recent episode of emergence. In northern Badoc Island, the apparent 'age inversion' or 'younging' of ages with increasing terrace elevation poses complexities in interpreting the coastal tectonics of the island.

## Terrace formation and emergence

From field observations, geomorphic analysis, and geochronologic data, the formation of Holocene coral terraces, RSL changes, and occurrence of a potentially extreme wave event in the last millennium are hypothesized. Between 7 and 6 ka ago, the mid-Holocene sea level highstand eroded the Holocene transgressive reef forming an erosional platform (T1) that is well preserved around Badoc Island; consequent emergence of the land or episodes of RSL fall then exposed the mid-Holocene corals. If the late Holocene (2727 ± 13 years BP) coral is attached or encrusted, emergence or uplift of the reef

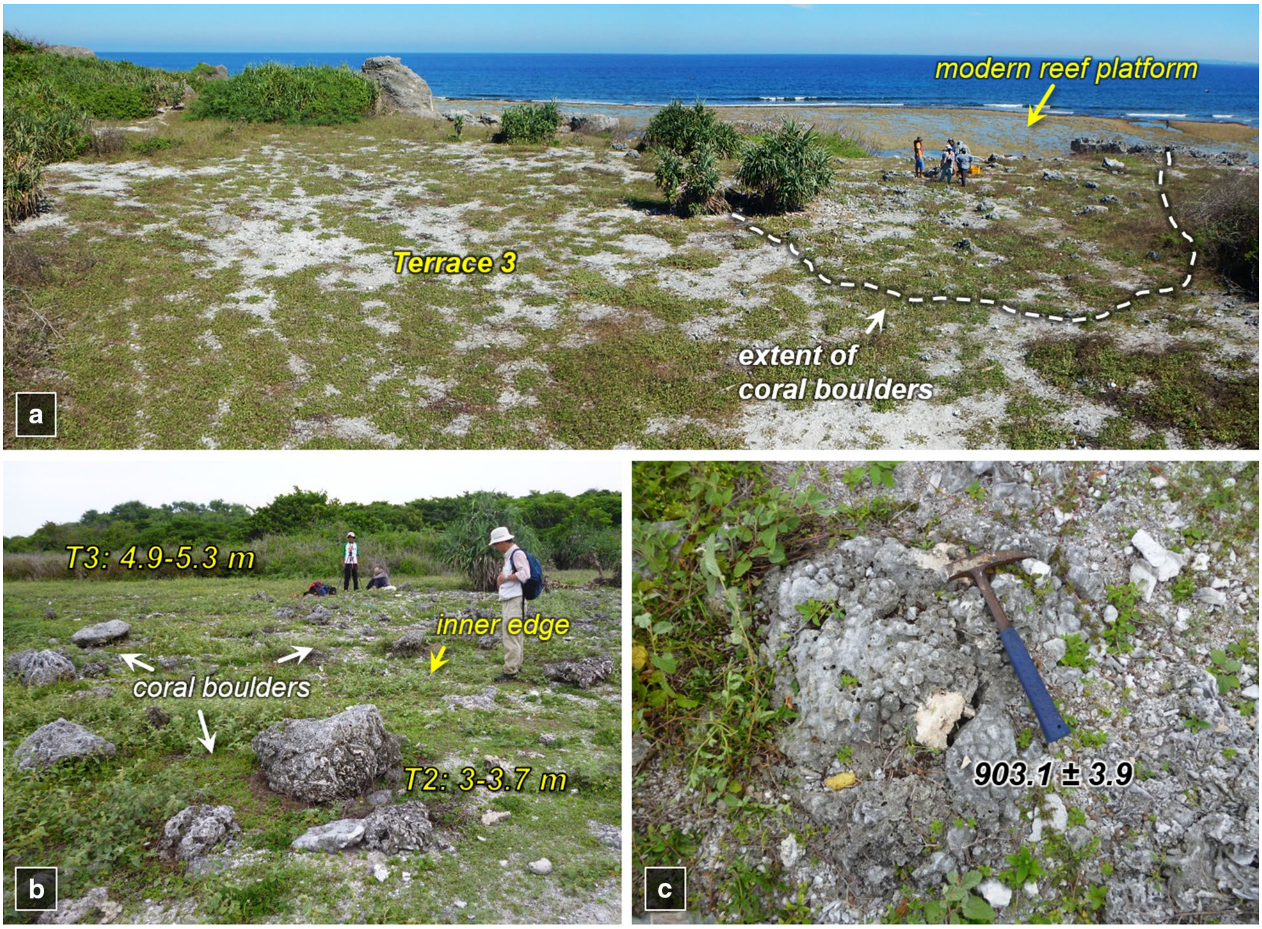


**Fig. 3** Representative photos of the survey site showing the occurrence and distribution of the coral boulders. **a** T3 rises to about 5 m amsl and is buried by sand, shells and shell fragments, and coral debris. Coral boulders are generally distributed close to the inner edge of T2 and just above the outer edge of T3. **b** Coral boulders on T2 and T3 are mostly individual corals, while the larger blocks are often cemented fragments of branching corals. **c** One of the young fossil corals, presumably *Porites*, sampled among the coral boulders on top of T3 yielded an age of 903.1 ± 3.9 years BP. A fossil coral sample nearby yielded an age of 945.1 ± 4.6 years BP

**Table 3 Geomorphologic data of survey site in Badoc Island, Ilocos Norte**

| Material | Height (m amsl)[a] | Occurrence | Age (year BP) relative to 1950 AD[b] | Initial $\delta^{234}U$ |
|---|---|---|---|---|
| Coral | 5 | Sand-covered terrace surface | 945.1 ± 4.6 | 147.6 ± 2.1 |
| Coral | 4.9 | Sand-covered terrace surface | 903.1 ± 3.9 | 143.8 ± 2.3 |
| Coral | 4.5 | Terrace riser | 2727 ± 13 | 146.6 ± 1.4 |
| Coral | 2.3 | Erosional reef platform | 6871.7 ± 22 | 148.1 ± 2.2 |

[a] Meters above mean sea level measured at the Currimao tide station (0.24 m)

[b] Age relative to chemistry date, corrections, and isotopic measurements (Cheng et al. 2013)

platform is inferred in which coseismic uplift of 4–5 m (i.e., to raise the terrace to its present position) must accompany the rupture of an offshore reverse fault. We further hypothesize that the apparent 'younging' of coral ages toward the upper terrace surfaces may imply a cycle of interseismic subsidence and coseismic uplift; however, such interpretation may only be tested when information from GPS and microatoll studies become available for coastal regions facing the Manila Trench.

We also postulate two possible scenarios of marine inundation to account for the occurrence of ~1000-year-old coral boulders on the upper terrace steps. Meter-scale coseismic uplift resulting from a significantly large offshore earthquake may have occurred in the last millennium and generated a tsunami that emplaced the coral boulders on the uplifted reef. The extreme wave scenario would seem more plausible as another fossil coral in cemented coral rubble from the mainland coast (about 1.5 km east of Badoc Island) yielded an age of 1,320 ± 5 years BP. The variable elevation of the ~1000-year-old corals from mainland Badoc (~2 m amsl) and Badoc Island (5 m amsl) implies that an overwash event would more likely account for the spatiotemporal distribution of the coral boulders, rather than differential uplift of the mainland coast and the island. If the young corals are assumed to be in situ, an almost 5-m-high coseismic uplift would require a large amount of slip and surface rupture area from either the Manila Trench megathrust- or nearby upper-plate fault. As the Philippines is also predisposed to extreme tropical cyclones, an alternative scenario entails emplacement of the coral boulders onto the terrace surface by an unusually strong typhoon.

## Historical extreme wave events across the Manila Trench and SCS regions

A recent catalog of tsunamis and seiches in the Philippines provides a summary and review of earthquake and tsunami reports derived from historical records, previous catalogs, and recent earthquake reports (Bautista et al. 2012). From 1589 to 2012, Bautista et al. (2012) list at least 11 tsunamigenic earthquakes which may have affected west Luzon in which some events may have originated from the Manila Trench. Of the 11 earthquake events, 5 were rated as having a positive certainty of tsunami occurrence (100%), while the other events have probable (75%), possible (50%), or doubtful (<25%) tsunami certainty (Fig. 1c; Table 4). These ratings were based on eyewitness accounts and quality of information (i.e., specific places affected, clear tsunami description). Historical tsunami data from the past decades to a few hundreds of years ago further reveal that wave inundation reached a maximum height of 2 m along the coasts of northwestern Luzon (Bautista et al. 2012).

The Philippines is also frequented by tropical cyclones (TC) which enter the country at an average of 19–20 TCs per year (Philippine Atmospheric, Geophysical and Astronomical Services Administration (PAGASA) 2008). While the 2013 Typhoon (TY) Haiyan (local name: Super Typhoon Yolanda) remains to be the deadliest typhoon in modern meteorologic records to hit the country, the 1881 Haiphong typhoon that devastated Vietnam is also reported to have severely damaged the Philippines leaving thousands of casualties [e.g., (Ribera et al. 2008; Terry et al. 2012); Table 4]. As the strongest landfalling tropical

**Table 4 Historical extreme wave events in west Luzon**

| Tsunami | | | | Deadliest and most destructive typhoons[a] | | | |
|---|---|---|---|---|---|---|---|
| Year | Magnitude (Ms) | Tsunami probability | Maximum tsunami height (m) | Year | Storm name (local name) | JMA scale | Saffir–Simpson scale (category) |
| 1677 | 7.3 | Possible | *No data* | 1867[b] | N/A | | |
| 1828 | 6.6 | Positive | 1 | 1881[b] | Haiphong | | |
| 1852 | 7.6 | Possible | *No data* | 1894[b] | N/A | | |
| 1862 | 6.1 | Doubtful | *No data* | 1897[b] | N/A | | |
| 1863 | 6.5 | Positive | 1 | 1984[b] | Ike (Nitang) | Typhoon | 4 |
| 1872 | 6.8 | Probable | *No data* | 1990 | Mike (Ruping) | Typhoon | 5 |
| 1924 | 7.0 | Positive | 1 | 1991[b] | Thelma (Uring) | Tropical storm | Tropical storm |
| 1983 | 6.5 | Positive | 1 | 1995 | Angela (Rosing) | Typhoon | 5 |
| 1934 | 7.6 | Positive | 2 | 2004[b] | Winnie | Tropical depression | N/A |
| 1937 | 7.5 | Positive | *No data* | 2006[b] | Durian (Reming) | Typhoon | 4 |
| 1939 | 6.5 | Doubtful | *No data* | 2008[b] | Fengshen (Frank) | Typhoon | 3 |
| 1990 | 7.8 | Positive | 2 | 2009 | Parma (Pepeng); Ketsana (Ondoy) | Typhoon | 4; 2 |
| 1999 | 6.8 | Positive | 1.5 | 2010 | Megi (Juan) | Typhoon | 5 |
| | | | | 2011 | Nesat (Pedring) | Typhoon | 4 |
| | | | | 2012[b] | Bopha (Pablo) | Typhoon | 5 |
| | | | | 2013[b] | Haiyan (Yolanda) | Typhoon | 5 |
| | | | | 2014 | Rammasun (Glenda) | Typhoon | 5 |

[a] Data from the National Disaster Risk Reduction and Management Council (NDRRMC) and compilation of Ribera et al. (2008) from Miguel Selga's *Catalogue of typhoons 1348–1934*

[b] Death toll more than 1000

cyclone, TY Haiyan generated a surge of 5–6 m (Tajima et al. 2014) and run-up as high as 15 m (Kennedy et al. 2017). In a recent assessment of storm surge vulnerable areas in the Philippines, storm surges from historical typhoons (1948–2013) that entered the Philippine Area of Responsibility (PAR) were modeled using the characteristics of TY Haiyan (Lapidez et al. 2015). Storm surge models reveal that coastal areas in the central Visayas, southern Luzon, and northeastern Mindanao are the most vulnerable to high storm surges, while the modeled storm surge heights along the west Luzon coastline range from 1 to 2 m (Lapidez et al. 2015). Prehistoric strong typhoons have also been reported to affect the west Luzon coast. Using coral lithofacies and chronology of a reef flat in La Union, the large wave event which possibly occurred 324 years BP was more likely a severe tropical cyclone event, but the occurrence of a tsunami was not completely ruled out (Gong et al. 2013).

Coral and stratigraphic data collected across the SCS region further provide evidence of an extreme wave event ~1000 years ago. From transported coral blocks and lagoon sediments in the southern SCS (Yongshu Reef), Yu et al. (2009) inferred a past strong storm or tsunami in AD 1064. Sand layers in lake sediment cores from the Xisha islands also indicate a sudden and high-energy event, potentially a tsunami, in AD 1024 (Sun et al. 2013). Among the historical strong wave events recorded in the SCS region, the AD 1071 event which affected Guangdong, China closely correlates with the stratigraphic data of Yu et al. (2009), Sun et al. (2013), and our dated coral samples (e.g., 945.1 ± 4.6 years BP or AD 1043–1051; 903.1 ± 3.9 years BP or AD 1000–1010) in Badoc Island. A potentially large coseismic uplift event in the last millennium is also inferred along west Luzon based on uplifted coral microatolls in La Union. Radiocarbon and $^{230}$Th/$^{234}$U dating of coral microatolls (0.8 m amsl) at Paraoir site reveal ages that range from 1.5 to 1.1 ka (Hosono 2003; Abigania 2011). However, recent analysis of historical tsunamis in written records and regional databases of the SCS region still present challenges in evaluating the validity of past tsunami events (Mak and Chan 2007; Lau et al. 2010).

## Wave inundation scenarios across the northern Manila Trench forearc region

To evaluate the process of emplaced coral boulders onto the 5-m-high terrace in Badoc Island, we performed simple numerical models to constrain a tsunami in the region. Two hypothetical source faults along the Manila Trench megathrust- and one upper-plate fault in the northern forearc region are modeled to constrain the transport and emplacement mechanism of Late Holocene corals in Badoc Island and nearby coasts (Fig. 4). For the megathrust model, we established the length of the potential source fault from the trench azimuth from 14°N to 18°N, while focal mechanism solutions were used to infer the orientation of the upper-plate fault. Fault widths were estimated using seismicity and coastal deformation patterns as interpreted from uplifted coral terraces in west Luzon [e.g., (Ramos and Tsutsumi 2010)]. The dip angle of the megathrust- and upper-plate faults was inferred from early geophysical data (e.g., gravity, seismic reflection) across the Manila Trench forearc region (Hayes and Lewis 1984) coupled with focal mechanism solutions (Fig. 1b). We then utilized the scaling relation of Murotani et al. (2013) and Wells and Coppersmith (1994) to estimate fault slip along the hypothetical megathrust- and upper-plate fault, respectively. For the megathrust fault model, a rupture along a 440-km × 120-km fault is calculated to have almost 3.5 m of slip and will generate a *Mw*8.5 earthquake. Subsidence of the west Luzon coastline is expected with any amount of slip along the megathrust and may therefore potentially amplify the impacts of the tsunami. Although available coastal geomorphic data in west Luzon are currently not sufficient to infer subsidence in the region, the possibility of interseismic and postseismic subsidence is high due to the region's active tectonic setting and exposure to subduction zone seismic cycles. To produce permanent uplift of the west Luzon coast to expose the reef terraces, rupture along an upper-plate fault in the forearc region is modeled. The upper-plate model is a 400-km × 80-km fault plane that is calculated to have almost 5 m of slip and will generate a *Mw*8.4 earthquake. The calculated slip and earthquake magnitude could potentially cause uplift of the west Luzon coast by as much as 1.5–2 m. In order to produce coastal uplift of about 3 m (i.e., height of the lowest emergent terraces), a larger amount of fault slip (i.e., 10 m) on the upper-plate fault is modeled and will produce a wave height of more than 5 m along the coasts of Badoc.

In both megathrust and upper-plate fault models, tsunami wave height (run-up height when wave approaches land) reaches more than 3 m high with inundation distance as far as 2 km along the coasts of Badoc (Fig. 5). It should be noted that the reported earthquake magnitudes resulting from the modeled hypothetical source fault rupture models are minimum values to generate a tsunami that will inundate Badoc Island and its mainland, and will potentially emplace coral boulders on surfaces that are a few meters high.

We further emphasize that the source fault, fault slip, and tsunami inundation models presented in this study are preliminary (i.e., values assigned to assess the potential effects of tsunamis) and will be refined as more geomorphologic, stratigraphic, and geophysical data become available. While emplacement of coral boulders by an

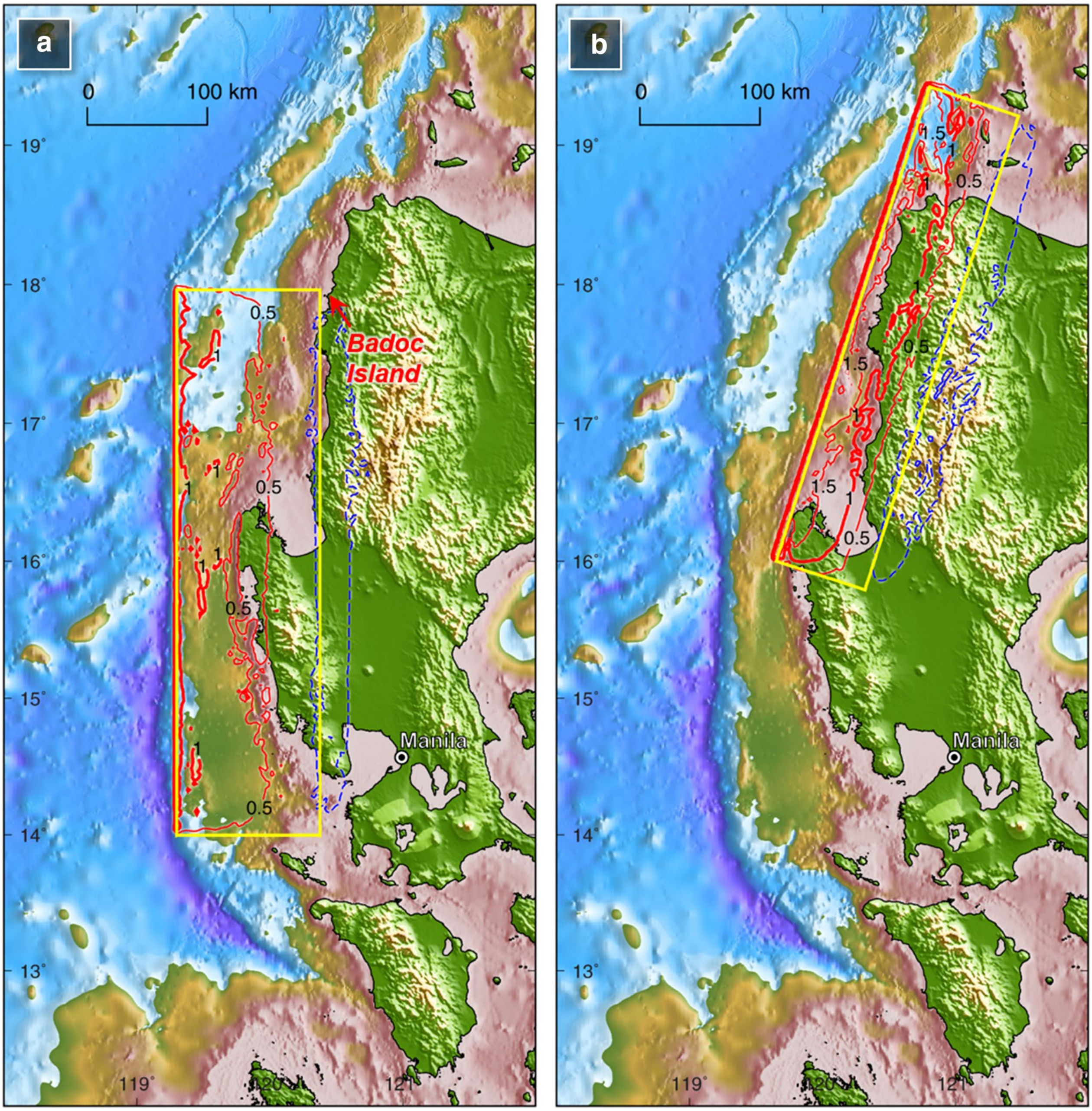


**Fig. 4** Hypothetical fault rupture scenarios showing uplift (*red*) and subsidence (*blue*) along west Luzon Island. Contours and *numbers* indicate amount of deformation in meters. **a** Fault rupture along the Manila Trench megathrust could lead to uplift of coastlines closer to the subduction zone (i.e., Pangasinan) but will largely cause subsidence along the west coasts of the Ilocos region. **b** Rupture of an offshore upper-plate reverse fault on the northern forearc region is modeled to approximate the deformation pattern of the lowest Holocene terraces in west Luzon

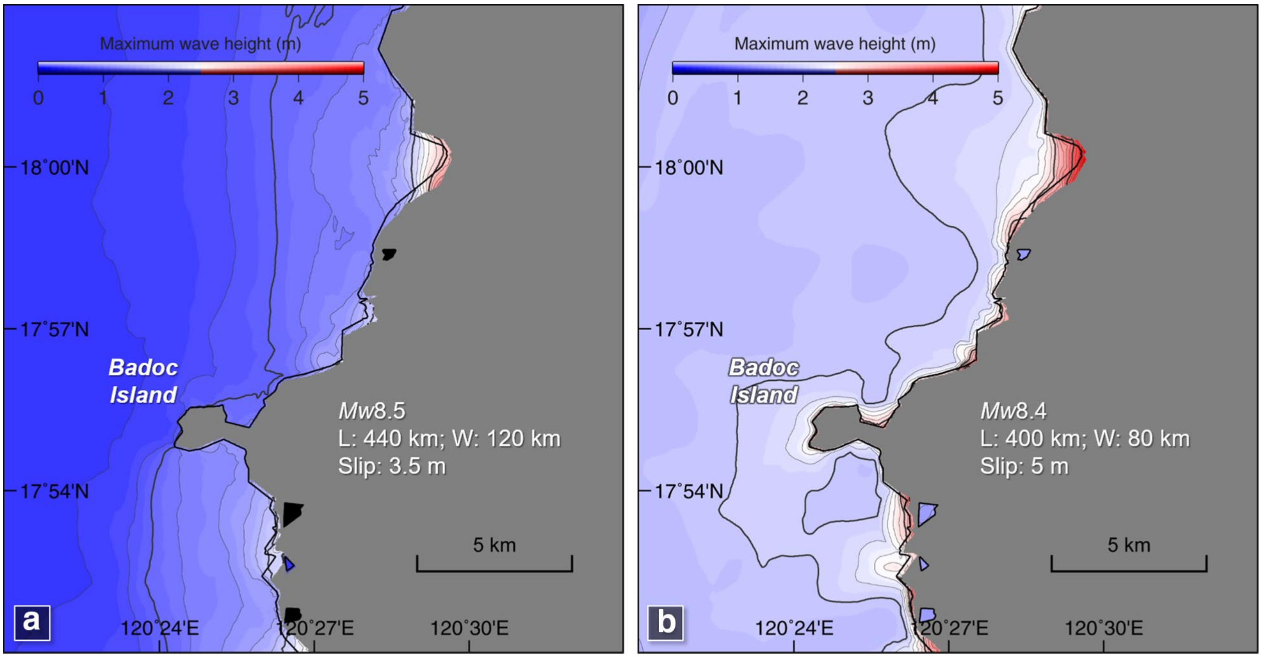


**Fig. 5** Tsunami inundation associated with **a** modeled megathrust and **b** upper-plate fault ruptures along the Manila Trench forearc region. Embayments and low-lying areas in Ilocos Norte are observed to be affected by waves more than 3 m high. Minimum earthquake magnitudes are estimated from inferred source fault parameters and amount of slip calculated from fault scaling relations. Contours in *bold lines* represent 1-m intervals. Note that the coastline resolution and extent of inundation are constrained by the resolution of the basemap used

unusually strong typhoon is also likely, modeled storm surge heights along west Luzon do not exceed 2 m even with Typhoon Haiyan characteristics [e.g., (Lapidez et al. 2015)].

## Conclusions

This study highlights the first and preliminary attempt to combine geomorphologic data and numerical models to constrain a prehistoric extreme wave event across the eastern SCS and Manila Trench forearc region. The occurrence of an extreme wave event about 1000 years ago is inferred based on the presence of young fossil corals on a ~5 m-high emergent coral platform in Badoc Island offshore west Luzon. The characteristics and distribution of ~1-ka-old coral boulders in Badoc Island and Badoc mainland suggest high-energy deposition and emplacement by overwash.

We used uplifted reef platforms to infer meter-scale coseismic uplift following a significantly large offshore earthquake that is also potentially tsunamigenic. Using scaling relations, preliminary seismotectonic models show that reverse slip of 5 m along a 400-km × 80-km upper-plate fault on the northern forearc region of the Manila Trench will generate a *Mw*8.4 earthquake and uplift of the west Luzon coastline by a few meters. To produce coastal uplift that will raise the lowest terraces to their present elevation, a larger amount of slip (10 m) is modeled. Meanwhile, a *Mw*8.5 megathrust earthquake along the Manila Trench on a 440-km × 120-km fault plane with pure reverse slip of 3.5 m is shown to cause subsidence of the west Luzon coastline and possibly increases the damage of wave inundation. Both source faults will lead to a tsunami wave height of more than 3 m and inundation distance as far as 2 km along the coasts of western and northern Luzon. While an unusually strong typhoon could also explain the overwash deposits, storm surge heights modeled for the west Luzon coastline do not exceed 2 m even with the characteristics of Typhoon Haiyan.

Although preliminary, the tsunami hypothesis is supported by rupture and inundation models (e.g., wave height) to account for the emplacement of coral boulders on an uplifted reef in Badoc Island. Future modeling of storm surges along the west Luzon coasts is recommended to further test the strong typhoon scenario. More importantly, this study highlights the vulnerability of coastal communities in west Luzon and surrounding cities across the SCS region to coastal hazards brought about by tsunamis and strong typhoons. By modeling past extreme wave events, we are able to assess the impacts of potentially similar events in the future and allow communities to prepare for worst case scenarios.

**Abbreviations**
NAMRIA: National Mapping and Resource Information Authority; MC-ICP-MS: multicollector inductively coupled plasma mass spectrometer; HISPEC: High-Precision Mass Spectrometry and Environment Change Laboratory; NTU: National Taiwan University; SCS: South China Sea; SRTM: Shuttle Radar Topography Mission; PHIVOLCS: Philippine Institute of Volcanology and Seismology.

**Authors' contributions**
NTR designed the study and led the writing of the manuscript, with inputs from KVM, HT, CCS and KS. NTR, KVM, and HT participated in the field surveys, data gathering, and interpretation of geomorphic data. CCS, KVM, YCC, and FD processed and measured $^{230}$Th ages of coral samples. NTR and KS performed the tsunami modeling, while KVM performed initial modeling of storm surge heights. All authors read and approved the final manuscript.

**Author details**
[1] National Institute of Geological Sciences, College of Science, University of the Philippines, Diliman, 1101 Quezon City, Philippines. [2] Department of Environmental Systems Science, Faculty of Science and Engineering, Doshisha University, Kyoto 610-0394, Japan. [3] High-Precision Mass Spectrometry and Environment Change Laboratory (HISPEC), Department of Geosciences, National Taiwan University, Taipei 10617, Taiwan, ROC. [4] Earthquake Research Institute, University of Tokyo, Tokyo 113-0032, Japan.

**Acknowledgements**
N. Ramos acknowledges the financial support of the Japan International Cooperation Agency Project Office for ASEAN University Network/Southeast Asia Engineering Education Development Network (JICA AUN/SEED-Net) through its Collaborative Research Program for Alumni Members (Project No. UP CRA1401). The authors are thankful to Hsun-Ming Hu of HISPEC Laboratory at the National Taiwan University for his assistance in $^{230}$Th dating of coral samples. N. Ramos performed the tsunami modeling and utilized the Earthquake Information Center (EIC) computer system through funding support from the Earthquake Research Institute (ERI), the University of Tokyo; A. Gusman, T. Ho, and M. Uehara are thanked for their scientific inputs and technical assistance. Field assistance was provided by L.F. Sarmiento, R.B. Mendoza, L.G. de Guia, and students of the GEAR (Geomorphology, Earthquakes, and Active Tectonics Research) and RWG (Rusurgent Working Group) laboratories at UP-NIGS. The Philippine Institute of Volcanology and Seismology (PHIVOLCS) and the National Mapping and Resource Information Authority (NAMRIA) are thanked for their provision of earthquake and high-resolution topographic data, respectively. The Mines and Geosciences Bureau (MGB) also provided support through provision of necessary permits for the samples. The authors also thank the local government officials of Ilocos Norte Province for their cooperation and logistical support; K.M. Cabacaba, J. Abat, and J.K. Suarez for their assistance in testing the hypothetical storm surge model through Delft 3D. The authors are grateful to the editor and three anonymous reviewers for their inputs that greatly improved the manuscript. Sections of this paper were presented at the 13th Annual Meeting of the Asia Oceania Geosciences Society in China, 35th International Geological Congress in South Africa, and 1st Meeting of the International Geoscience Programme (IGCP) Project 639 in Oman with travel support from the University of the Philippines Office of the Vice President for Academic Affairs (UP OVPAA) and IGCP. This paper is a contribution to IGCP Project 639: Sea Level Change from Minutes to Millennia.

**Competing interests**
The authors declare that they have no competing interests.

**Availability of data and materials**
The datasets supporting the conclusions of this article are included within the article.

**Funding**
This research was supported by the Japan International Cooperation Agency Project Office for ASEAN University Network/Southeast Asia Engineering Education Development Network (JICA AUN/SEED-Net) through its Collaborative Research Program for Alumni Members (Project No. UP CRA 1401). U-Th dating at the HISPEC was supported by Taiwan ROC-MOST and NTU Grants (104-2119-M-002-003, 105-2119-M-002-001, and 105R7625 to CCS). The Earthquake Research Institute, the University of Tokyo supported the research activities of N. Ramos in Japan through its research fellowship program.

## Publisher's Note
Springer Nature remains neutral with regard to jurisdictional claims in published maps and institutional affiliations.

Received: 2 December 2016 Accepted: 2 May 2017
Published online: 10 May 2017

**References**
Abigania MIT (2011) Paleoseismicity and vertical land movements from the morphology of Holocene coral microatolls at Paraoir, La Union, Philippines. M.Sc.Thesis (unpublished), University of the Philippines-Diliman, Quezon City, Philippines, p 132
Baba T, Takahashi N, Kaneda Y, Inazawa Y, Kikkojin M (2014) Tsunami inundation modeling of the 2011 Tohoku earthquake using three-dimensional building data for Sendai, Miyagi Prefecture, Japan, Tsunami events and lessons learned. Adv Nat Technol Hazards Res 35:89–98. doi:10.1007/978-94-007-7269-4-3
Baba T, Takahashi N, Kaneda Y, Ando K, Matsuoka D, Kato T (2015a) Parallel implementation of dispersive tsunami wave modeling with a nesting algorithm for the 2011 Tohoku tsunami. Pure Appl Geophys 172(12):3455–3472. doi:10.1007/s00024-015-1049-2
Baba T, Ando K, Matsuoka D, Hyodo M, Hori T, Takahashi N, Obayashi R, Imato Y, Kitamura D, Uehara H, Kato T, Saka R (2015b) Large-scale, high-speed tsunami prediction for the great Nankai trough earthquake on the K computer. Int J High Perform Comput Appl 30(1):71–84. doi:10.1177/1094342015584090
Bautista MLP, Bautista BC, Salcedo JC, Narag IC (2012) Philippine tsunamis and seiches (1589–2012): A catalogue of tsunami events in the Philippines. Philippine Institute of Volcanology and Seismology (PHIVOLCS), Quezon City, Philippines, p 111
Besana GM, Tanioka Y, Ando M, Mirabueno MH, Manahan J, De Ocampo J, Perez JS, Bautista BC (2004) The May 17, 1992 earthquakes in southeastern Philippines. Geophys Res Lett 31:L24618. doi:10.1029/2004GL020917
Cheng H, Edwards RL, Shen CC, Polyak VJ, Asmerom Y, Woodhead J, Hellstrom J, Wang Y, Kong X, Spötl C, Wang X, Alexander ECJ (2013) Improvements in 230Th dating, 230Th and 234U half-life values, and U-Th isotopic measurements by multi-collector inductively coupled plasma mass spectrometry. Earth Planet Sci Lett 371–372(2013):82–91. doi:10.1016/j.epsl.2013.04.006
Dao MH, Tkalich P, Chan ES, Megawati K (2009) Tsunami propagation scenarios in the South China Sea. J Asian Earth Sci 36:67–73. doi:10.1016/j.jseaes.2008.09.009
Hayes DE, Lewis SD (1984) A geophysical study of the Manila Trench, Luzon, Philippines 1. Crustal structure, gravity, and regional tectonic evolution. J Geophys Res 89(Bll):9171–9195. doi:10.1029/JB089iB11p09171
Gong SY, Wu TR, Siringan FP, Lin K, Shen CC (2013) An abrupt backreef infilling in a Holocene reef, Paraoir, Northwestern Luzon, Philippines. Coral Reefs 32(1):293–303. doi:10.1007/s00338-012-0982-0
Goto K, Miyagi K, Kawamata H, Imamura F (2010) Discrimination of boulders deposited by tsunamis and storm waves at Ishigaki Island, Japan. Mar Geol 269:34–45. doi:10.1016/j.margeo.2009.12.004
Hiess J, Condon DJ, McLean N, Noble SR (2012) $^{238}$U/$^{235}$U Systematics in terrestrial uranium-bearing minerals. Science 335(6076):1610–1614. doi:10.1126/science.1215507
Hosono Y (2003) Relative sea level change and uplift timing from geologic history of emerged Holocene reef terrace in the Northwest Luzon, Philippine islands. Master's Thesis, Kanazawa University, Japan, p 75
Huang Z, Wu TR, Tan SK, Megawati K, Shaw F, Liu X, Pan TC (2009) Tsunami hazard from the subduction megathrust of the South China Sea: part II. Hydrodynamic modeling and possible impact on Singapore. J Asian Earth Sci 36:93–97. doi:10.1016/j.jseaes.2008.08.007
Intergovernmental Panel on Climate Change (IPCC) (2013). Climate Change 2013: the physical science basis. Contribution of Working Group I to the Fifth Assessment Report of the Intergovernmental Panel on Climate Change. In: Stocker TF, Qin, D, Plattner GK, Tignor M, Allen SK, Boschung J, Nauels A, Xia Y, Bex V, Midgley PM (eds) Cambridge University Press, Cambridge, United Kingdom and New York, NY, USA, p 1535. doi:10.1017/CBO9781107415324

Jaffey AH, Flynn KF, Glendenin LE, Bentley WC, Essling AM (1971) Precision measurement of half-lives and specific activities of 235U and 238U. Phys Rev C 4(5):1889. doi:10.1103/PhysRevC.4.1889
Jakeman JD, Nielsen OM, Vanputten K, Mleczeko R, Burbidge D, Horspool N (2010) Towards spatially distributed quantitative assessment of tsunami inundation models. Ocean Dyn 60(5):1115–1138. doi:10.1007/s10236-010-0312-4
Jara-Muñoz J, Melnick D, Brill D, Strecker MR (2015) Segmentation of the 2010 Maule Chile earthquake rupture from a joint analysis of uplifted marine terraces and seismic-cycle deformation patterns. Quat Sci Rev 113(2015):171–192. doi:10.1016/j.quascirev.2015.01.005
Kennedy AB, Mori N, Yasuda T, Shimozono T, Tomiczek T, Donahue A, Shimura T, Imai Y (2017) Extreme block and boulder transport along a cliffed coastline (Calicoan Island, Philippines) during Super Typhoon Haiyan. Mar Geol 383(2017):65–77. doi:10.1016/j.margeo.2016.11.004
Lapidez JP, Tablazon J, Dasallas L, Gonzalo LA, Cabacaba KM, Ramos MMA, Suarez JK, Santiago J, Lagmay AMF, Malano V (2015) Identification of storm surge vulnerable areas in the Philippines through the simulation of Typhoon Haiyan-induced storm surge levels over historical storm tracks. Nat Hazards Earth Syst Sci 15:1473–1481. doi:10.5194/nhess-15-1473-2015
Lau AYA, Switzer AD, Dominey-Howes D, Aitchison JC, Zong Y (2010) Written records of historical tsunamis in the northeastern South China Sea-challenges associated with developing a new integrated database. Nat Hazards Earth Syst Sci 10:1793–1806. doi:10.5194/nhess-10-1793-2010
Li L, Switzer AD, Chan CH, Wang Y, Weiss R, Qiu Q (2016) How heterogeneous coseismic slip affects regional probabilistic tsunami hazard assessment: a case study in the South China Sea. J Geophys Res Solid Earth 121:6250–6272. doi:10.1002/2016JB013111
Liu PLF, Wang X, Salisbury AJ (2009) Tsunami hazard and early warning system in South China Sea. J Asian Earth Sci 36:2–12. doi:10.1016/j.jseaes.2008.12.010
Mak S, Chan LS (2007) Historical tsunamis in South China. Nat Hazards 43:147–164. doi:10.1007/s11069-007-9113-6
May SM, Engel M, Brill D, Cuadra C, Lagmay AMF, Santiago J, Suarez JK, Reyes M, Brückner H (2015) Block and boulder transport in Eastern Samar (Philippines) during Supertyphoon Haiyan. Earth Surf Dyn 3:543–558. doi:10.5194/esurf-3-543-2015
Megawati K, Shaw F, Sieh K, Huang Z, Wu TR, Lin Y, Tan SK, Pan TC (2009) Tsunami hazard from the subduction megathrust of the South China Sea: part I. Source characterization and the resulting tsunami. J Asian Earth Sci 36:13–20. doi:10.1016/j.jseaes.2008.11.012
Murotani S, Satake K, Fujii Y (2013) Scaling relations of seismic moment, rupture area, average slip, and asperity size for M ~ 9 subduction-zone earthquakes. Geophys Res Lett 40:5070–5074. doi:10.1002/grl.50976
National Mapping and Resource Information Authority (NAMRIA) (2016) Philippines tide and current tables 2016. Oceanographic Survey Division, Coast and Geodetic Survey Department, Manila, Philippines, p 412
Nguyen PH, Bui QC, Vu PH, Pham TT (2014) Scenario-based tsunami hazard assessment for the coast of Vietnam from the Manila Trench source. Phys Earth Planet Inter 236(2014):95–108. doi:10.1016/j.pepi.2014.07.003
Okada Y (1985) Surface deformation due to shear and tensile faults in a half-space. B Seismol Soc Am 75(4):1435–1454
Philippine Atmospheric, Geophysical and Astronomical Services Administration (PAGASA) (2008) Member Report to the ESCAP/WMO Typhoon Committee, 41st Session. Chiang Mai, Thailand, p 38
Philippine Institute of Volcanology and Seismology (PHIVOLCS) (2015) Distribution of active faults and Trenches (Map). Department of Science and Technology, Quezon City, Philippines. http://www.phivolcs.dost.gov.ph
Ramos NT, Tsutsumi H (2010) Evidence of large prehistoric offshore earthquakes deduced from uplifted Holocene marine terraces in Pangasinan Province, Luzon Island, Philippines. Tectonophysics 495(3–4):145–158. doi:10.1016/j.tecto.2010.08.007
Ribera P, Garcia-Herrera R, Gimeno L (2008) Historical deadly typhoons in the Philippines. Weather 63(7):194–199
Ruangrassamee A, Saelem N (2009) Effect of tsunamis generated in the Manila Trench on the Gulf of Thailand. J Asian Earth Sci 36:56–66. doi:10.1016/j.jseaes.2008.12.004
Saito T, Satake K, Furumura T (2010) Tsunami waveform inversion including dispersive waves: the 2004 earthquake off Kii Peninsula, Japan. J Geophys Res 115:B06303. doi:10.1029/2009JB006884
Salcedo JC (2014) Study on earthquake source parameters for subduction zone events causing tsunamis in and around the Philippines: its application and results. Abstracts of the 10th General Assembly of the Asian Seismological Commission, Makati City, Philippines, p 124
Satake K (2002) Tsunamis. In: Lee WHK, Kanamori H, Jennings PC, Kisslinger C (eds) International handbook of earthquake and engineering seismology, part A. Academic Press, California, pp 437–451
Shen CC, Cheng H, Edwards RL, Moran SB, Edmonds HN, Hoff JA, Thomas RB (2003) Measurement of attogram quantities of 231 Pa in dissolved and particulate fractions of seawater by isotope dilution thermal ionization mass spectroscopy. Anal Chem 75:1075–1079
Shen CC, Li KS, Sieh K, Natawidjaja D, Cheng H, Wang X, Edwards RL, Lam DD, Hsieh YT, Fan TY, Meltzner AJ, Taylor FW, Quinn TM, Chiang HW, Kilbourne KH (2008) Variation of initial $^{230}$Th/$^{232}$Th and limits of high precision U-Th dating of shallow-water corals. Geochim Cosmochim Acta 72(2008):4201–4223. doi:10.1016/j.gca.2008.06.011
Shen CC, Wu CC, Cheng H, Edwards RL, Hsieh YT, Gallet S, Chang CC, Li TY, Lam DD, Kano A, Hori M, Spötl C (2012) High-precision and high resolution carbonate 230Th dating by MC-ICP-MS with SEM protocols. Geochim Cosmochim Acta 99:71–86. doi:10.1016/j.gca.2012.09.018
Smith WHF, Sandwell DT (1997) Global seafloor topography from satellite altimetry and ship depth soundings. Science 277:1957–1962. doi:10.1126/science.277.5334.1956
Sun L, Zhou X, Huang W, Liu X, Yan H, Xie Z, Wu Z, Zhao S, Shao D, Yang W (2013) Preliminary evidence for a 1000-year-old tsunami in the South China Sea. Sci Rep 3:1655. doi:10.1038/srep01655
Switzer AD, Mamo AL, Dominey-Howes D, Strotz LC, Courtney C, Jones BG, Haslett SK, Everett DM (2010) On the possible origins of an unusual (Mid to Late Holocene) Coastal Deposit, Old Punt Bay, South-East Australia. Geogr Res 49(4):408–430. doi:10.1111/j.1745-5871.2011.00700.x
Tajima Y, Yasuda T, Pacheco BM, Cruz EC, Kawasaki K, Nobuoka H, Miyamoto M, Asano Y, Arikawa T, Ortigas N, Aquino R, Mata W, Valdez J, Briones F (2014) Initial report of JSCE-PICE joint survey on the storm surge disaster caused by Typhoon Haiyan. Coast Eng J 56(1):1450006
TaniokaY Satake K (1996) Tsunami generation by horizontal displacement of ocean bottom. Geophys Res Lett 23:861–864. doi:10.1029/96GL00736
Terry JP, Etienne S (2014) Potential for timing high-energy marine inundation events in the recent geological past through age-dating of reef boulders in Fiji. Geosci Lett 2014:1–14
Terry JP, Goff J (2012) Natural hazards in the Asia-Pacific region: recent advances and emerging concepts. Geol Soc London Spec Publ 361:1–2. doi:10.1144/SP361.1
Terry JP, Winspear N, Cuong TQ (2012) The 'terrific Tongking typhoon' of October 1881—implications for the Red River Delta (northern Vietnam) in modern times. Weather 67(3):72–75
Tsutsumi H, Perez JS (2013) Large-scale active fault map of the Philippine fault based on aerial photograph interpretation. Active Fault Res 39:29–37
Villarin JT, Algo JL, Cinco TA, Cruz FT, de Guzman RG, Hilario FD, Narisma GT, Ortiz AM, Siringan FP, Tibig LV (2016). 2016 Philippine Climate Change Assessment (PhilCCA): the physical science basis. The Oscar M. Lopez Center for Climate Change Adaptation and Disaster Risk Management Foundation Inc. and Climate Change Commission, p 108
Wells DL, Coppersmith KJ (1994) New empirical relationships among magnitude, rupture length, rupture width, rupture area, and surface displacement. B Seismol Soc Am 84(4):974–1002
Wu TR, Huang HC (2009) Modeling tsunami hazards from Manila trench to Taiwan. J Asian Earth Sci 36:21–28. doi:10.1016/j.jseaes.2008.12.006
Yu KF, Zhao JX, Collerson KD, Shia Q, Chen TG, Wang PX, Liu TS (2004) Storm cycles in the last millennium recorded in Yongshu Reef, southern South China Sea. Palaeogeogr Palaeoclim Palaeoecol 210:89–100. doi:10.1016/j.palaeo.2004.04.002
Yu KF, Zhao JX, Shi Q, Meng QS (2009) Reconstruction of storm/tsunami records over the last 4000 years using transported coral blocks and lagoon sediments in the southern South China Sea. Quat Int 195(2009):128–137. doi:10.1016/j.quaint.2008.05.004